

NITROGEN EFFECT ON THE SURFACE AND OPTICAL PROPERTIES OF CUBIC AND HEXAGONAL BN NANO LAYERED THIN FILMS DEPOSITED BY RF SPUTTERING METHOD

Suat PAT

Physics Department, Eskisehir Osmangazi University, 26480, Eskişehir, Turkey

ABSTRACT

In this study, the influence of N₂ gas concentration on the surface and optical properties of BN thin films was investigated. A cubic BN phase, from the hexagonal structure, was produced by nitrogen changing during the deposition process. All BN thin films were deposited on glass substrates by the reactive radio frequency magnetron sputtering method with argon / nitrogen (ratios of 3:7, 1:1 and 4:1) gas mixtures. For the determination of the surface and optical properties of these two phases, field emission scanning electron microscopy, wavelength dispersive x-ray spectroscopy, atomic force microscopy, UV-Vis spectrophotometry, tensiometry, and interferometry tools were used. According to the results, the deposited films are homogeneous, compact nano-structured, and hydrophobic. Perfect stoichiometric ratios were obtained for the deposited samples. Phase transitions to cubic phase from hexagonal BN crystal system were only obtained by N₂ gas concentration.

Keywords: Nano-thick BN layer; Cubic BN; Hexagonal BN; Surface properties; Optical properties

RF SICRATMA METODU İLE DEPOLANMIŞ KÜBİK VE HEGZAGONAL BN NANO TABAKALANDIRILMIŞ İNCE FİLMLEİN YÜZEY VE OPTİKSEL ÖZELLİKLERİNE AZOT ETKİSİ

ÖZET

Bu çalışmada, BN ince filmlerin yüzey ve optiksel özelliklerine N₂ gaz konsantrasyonunun etkisi araştırılmıştır. Hegzagonal yapıdan kubik BN fazı, depolama esnasında azot gazı konsantrasyonu değişimi ile üretilmiştir. Tüm BN ince filmler reaktif radyo frekans manyetik sıçratma metodu kullanarak argon/azot (3:7, 1:1 ve 4:1 oranlarında) gaz karışımlarıyla cam alt taşlar üzerine üretilmişlerdir. Bu iki fazın yüzey ve optiksel özelliklerinin belirlenmesi için, dalgaboyu dağılım X-ışın spektroskopisi, atomik kuvvet mikroskopu, UV-Vis spektrofotometre, tensiyometre ve interferometre ölçüm cihazları kullanılmıştır. Sonuçlara göre, depolanmış ince filmler homojen, sıkı yapılı, nano yapılı ve hidrofobiktir. Mükemmel sitokiyometrik oranlar depolanmış örneklerde elde edilmiştir. Hegzagonal BN kristal sistemden kubik faza geçiş N₂ gaz konsantrasyonunun değişimi ile elde edilmiştir.

Anahtar Kelimeler: Nano kalınlıklı BN tabakası; Kübik BN; Hegzagonal BN; Yüzey özellikleri; Optiksel özellikler

1. INTRODUCTION

Boron nitride (BN) displays a wide band gap of 6.2 eV [1–3]. It is a ceramic material and it has an exceptional chemical and thermal stability. BN is used as a III-V compound. BN layers are used for high-temperature dielectrics, electron field emitters, coatings for tribological applications, and interfacial layers for optoelectronic devices [4–6]. However, the synthesis of high quality BN films is generally implemented at relatively high temperatures that are marginally compatible with solar cell manufacture [7–11]. Moreover, boron nitride is a dry lubricant. A BN material shows interesting properties, which are changed with respect to the crystal structures.

In this paper, the influences of the N₂ concentration on the optical, surface and crystallographic properties of nanostructured BN thin films are presented. The microstructure, phase analysis, surface

compositions, 2D surface images, contact angle (CA) and surface free energies (SFE), transmittance and refractive indices were investigated by changing the N₂ concentration.

2. EXPERIMENTAL DETAILS

The reactive RF sputtering system was introduced in previously published papers [9–10]. The RF power supply of 13.56 MHz was used to generate plasma. The diameter of the sputtering target is 2 inches in hexagonal BN and the purity of the target is higher than 99.5%. The distance between the sputter target and the glass substrate was adjusted to 30 mm. The gas mixture rate of Ar:N₂ was adjusted to (3:7), (1:1) and (4:1). These samples were labelled as *sample 1*, *sample 2* and *sample 3*, respectively. The working pressure was approximately 300 mTorr (approximately 40 Pa). The RF power was 250 W. The deposition time for all samples was 70 min. The pressure, applied RF power, and gas composition are the most important parameters in the RF sputtering process [3,6].

3. EXPERIMENTAL RESULTS

The thickness of the films was measured as approximately 50 nm, 100 nm and 120 nm for the gas mixing rates of *sample 1*, *sample 2* and *sample 3*, respectively. The Lorentz model was used to determine the thickness. Measurements were realized by the Filmetrics F20 thin film thickness measurement system as an interferometer.

PANalytical Empyrean XRD was used for microstructure and crystallographic data of BN layers deposited on glass substrates. Score analyses were realized. The score was calculated for all candidates to determine how well they match the experimental data. A high score indicates a better match with the experimental data. All three XRD spectra are polycrystalline in form. The XRD patterns are shown in Figure 1. The crystal systems are hexagonal and cubic in structure. These crystal structures were changed by the nitrogen concentration. Cubic and hexagonal structures were determined at the gas concentration of *sample 1*. The cubic structure of BN is the strongly dominant phase compared with the hexagonal phase in *sample 1*. The *score* percentage of the cubic phase of the deposited layer at the *sample 1* concentration is found to be 90%. With the gas composition of *sample 2* and *sample 3*, the amounts of the hexagonal phase of the BN are nearly the same. But, these differences were due to the nitrogen concentrations. The stoichiometric ratios of all of the samples were 1. This ratio was obtained from XRD analysis. The detailed XRD results are seen in Table 1.

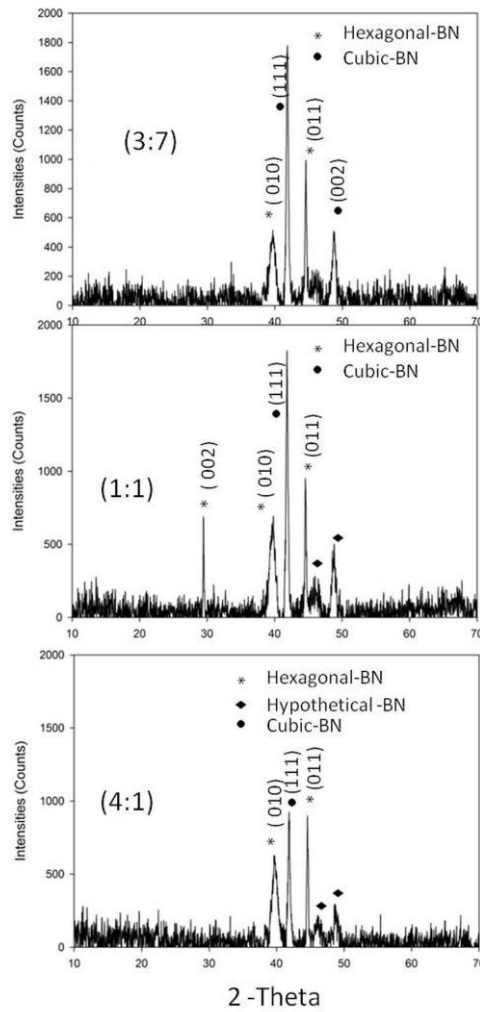


Figure 1. XRD spectra of the samples

The Debye-Scherrer equation is used to determine the grain size. This equation can be written as:

$$D = \frac{K\lambda}{\beta \cos\theta} \quad (1)$$

D is the mean size of the crystallite. The calculated mean crystallite sizes were added to Table 1. The real crystallite size is equal to or smaller than the calculated values. K is the shape factor (K is equal to 0.9). λ is the x-ray wavelength used. β is the line broadening at half maximum intensity value. This value is called the full width at half maximum (FWHM). θ is the Bragg angle [12–15]. The Debye-Scherrer equation is a limited equation for the grain size. It can be used only for nanocrystalline materials. The grain size must be smaller than 100 nm. For larger grains, it is not suitable.

High pressure is an important factor in the production of cubic phase BN from hexagonal form BN [16]. Also, cubic BN is related with argon ion energy [17]. The boron–nitrogen recombination process was realized at higher pressure [17]. The cubic BN ratio in the deposited film increases with the deposition temperature [18]. The deposition temperature is related with the N_2 concentration in the mixed gas. The cubic BN ratio [19] content decreases with increasing N_2 pressure [19].

Table 1. Detailed XRD results for the produced BN samples

	2- Theta (2 θ)	Intensity (Counts)	FWFM (2 θ)	d space (Å)	Relative intensity	Grain size (nm)	
Sample 1 (Argon/Nitrogen) (3:7)	39.6870	469.19	0.8187	2.27112	26.74	10	
	41.8815	1754.4	0.2303	2.15706	100	37	
	44.5950	932.72	0.1791	2.03191	53.16	50	
	48.7978	462.42	0.4093	1.86628	26.36	20	
	Reference code		Compound name		Stoichiometric rate		Score
	98-016-2870	Hexagonal	Boron Nitride	B1 N1	7		
	98-005-6315	Cubic	Boron Nitride	B1 N1	69		
Sample 2 (Argon/Nitrogen) (1:1)	39.6999	595.07	0.614	2.27042	65.62	13	
	41.8163	906.88	0.1535	2.16027	100	55	
	44.5966	901.87	0.2047	2.03183	99.45	42	
	46.0579	242.01	0.8187	1.97072	26.69	10	
	48.8300	225.4	0.614	1.86513	24.85	14	
	Reference code		Compound name		Stoichiometric rate		Score
	98-016-2870	Hexagonal	Boron Nitride	B1 N1	5		
Sample 3 (Argon/Nitrogen) (4:1)	39.6625	768.66	0.7164	2.27247	85.17	12	
	41.8468	902.46	0.2047	2.15876	100	42	
	44.5976	754.13	0.2303	2.03179	83.56	37	
	48.8174	214.95	0.7164	1.86558	23.82	12	
	Reference code		Compound name		Stoichiometric rate		Score
	98-016-2870	Hexagonal	Boron Nitride	B1 N1	5		

The size of the crystals is approximately 20–30 nm, as shown in Figure 1. These results show very good accordance with the Debye-Scherrer calculations and other measurements. A scanning electron microscope with a field emission cathode (Zeiss Supra 40VP) was used for surface imaging. A nearly homogeneous surface was obtained. The FESEM images of the deposited samples are illustrated in Figure 2. The dimensions of the grains and local agglomerations in the images are seen clearly. The FESEM images are distinct from each other. The surface images and microstructures were changed by the N₂ concentration.

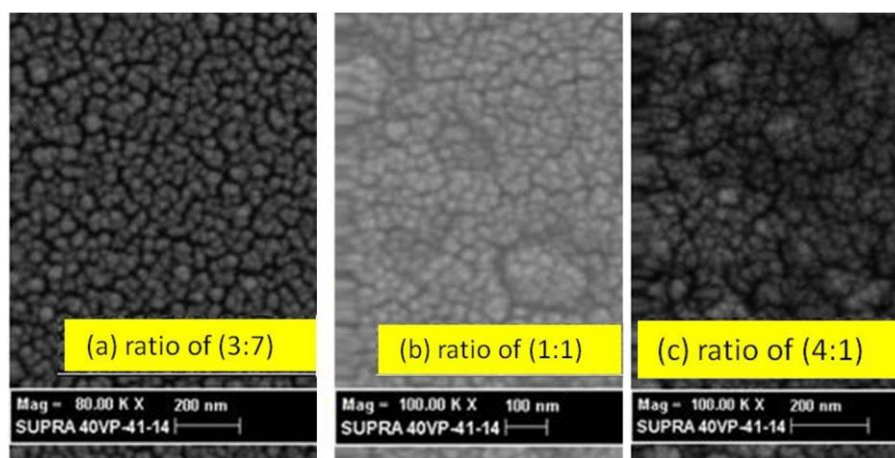


Figure 2. FESEM images of the sample surfaces

Ambios Q-Scope atomic force microscopy was used for the surface imaging. The images obtained are given in Figure 3 at the same imaging scale as for the FESEM images. As shown in Figures 2 and 3, the dimensions of the grains and local agglomeration on the surface of the samples are approximately 20–30 nm. These are nearly the same size in the FESEM image. The grains are seen more clearly in the phase images. The average surface roughness (RMS) was calculated as 1.16 nm for *sample 1*, 4 nm for *sample 2* and 1 nm for *sample 3* from the 40 parallel lines of the surface using the AFM Q-scope operating software. The yellow and white are hills and peaks of the surface.

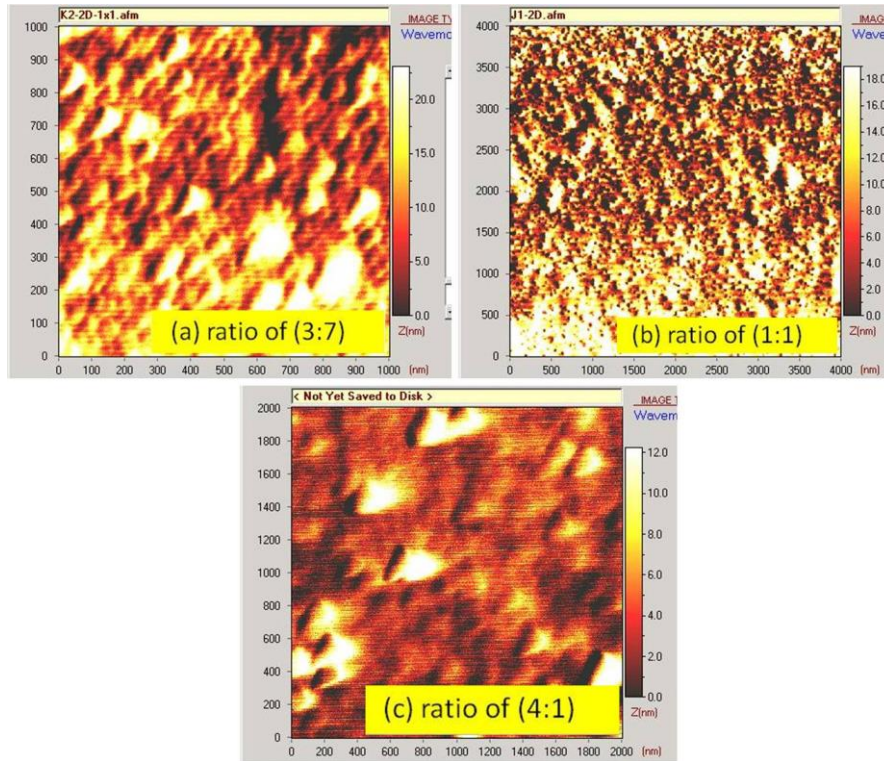


Figure 3. AFM images of the deposited layers

A BN thin film with nano-metric thickness has high transparency [1–8]. A UV-Vis spectrophotometer was used for the transmittance and absorbance measurements. Transmittance spectra measurement of the layer was realized by a UNICO 4802 UV-Vis double beam spectrophotometer in the spectral range of 300–1100 nm. The transparency of the film will increase dramatically according to the N_2/Ar ratio [3]. Graphs of reflection versus wavelength (nm) are shown in Figure 4a. This film shows anti-reflective properties at approximately 550 nm. The reflection value suddenly drops to lower values. According to the anti-reflection calculations, the film thickness is calculated to be 70 nm. This is nearly the same value as that obtained with the Lorentz model using the Filmetrics F20 thin film thickness measurement system. The values of the refractive indices varied in the measured range of 1.96–2.10 in the optical region. These refractive index values are shown in Figure 4b. Band gap values are calculated from the refractive index values. Considering these calculations, the obtained BN film shows ceramic properties as its band gap is calculated to be approximately 5.8 eV. This value is in good agreement with the literature [9]. An equation for the band gap energy is as follows:

$$\frac{n^2-1}{n^2+2} = 1 - \sqrt{Eg/20} \quad (2)$$

where n is the refractive index and Eg is the band gap energy of the sample [11, 13].

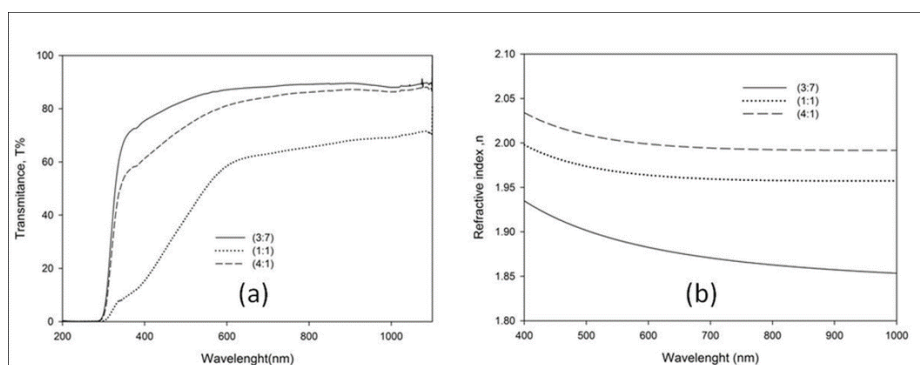


Figure 4. (a) Transmittance and (b) refractive index spectra of BN layers

The surface free energies of BN thin films were calculated from the contact angle measured by an Attension Theta Lite tensiometer. Water, ethylene glycol, diiodomethane, and formamide liquids were used as a heavy phase for surface free energy (SFE) experiments. The SFE of the solid is proportional to the surface tension. SFE is the proportion of surface tension for the solids. The method used and the results obtained are shown in Table 2. The minimum value of the measured contact angle (CA) was measured as over 100° for water. The CA for the other heavy liquids is summarized in Table 2, which shows that BN thin films are hydrophobic. According to the results of the CA analyses, nearly all the drops of liquid are pushed from the surface. It was found that the CA and SFE are not strongly dependent on the BN crystal phases. The SFEs of the films are calculated by various methods. These measurements are seen in Table 2. According to the literature, the SFE values obtained are very low. Moreover, the obtained roughness of the films is lower. Consequently, a lower SFE value shows a lower roughness and lower surface area. We concluded that the roughness of the surface plays a substantial role in the values of the contact angle and SFE. The SFE of a solid is proportional to the surface tension of the liquid. Surface roughness, calculated by AFM, influences the CA and SFE of the sample surfaces. When the AFM roughness increased, the CA dropped to a lower value. Relevant results for the relation between the CA and AFM roughness were obtained in [20]. An interesting result was found for the CA values for the four different heavy media, where all the calculated values were very high.

Table 2. Contact angle (CA) and surface free energy (SFE) values for different liquids

	Sample	1	2	3
Heavy media CA ($^\circ$)	Water	109	100	106
	Ethylene Glycol	110	118	130
	Formamide	115	102	94
	Di-iodomethane	107	96	88
Surface free energy (SFE) (mJ/m^2)	Acid-base	3	1	7
	Equation of state	10	12	13
	Owrk/fowkes	7	10	11
	Wu	12	15	17

4. CONCLUSION

In summary, BN thin films were deposited as nano-sheets or ultra-thin film on glass substrates for determination of their optical and surface properties. For the deposition process, high-pressure RF reactive magnetron sputtering was used. The deposited thin films showed improved properties such as homogeneity, purity, and low roughness and hydrophobicity and nano-crystallinity. According to XRD analysis, perfect stoichiometric ratios were obtained for all samples. All the stoichiometric rates are 1 for the B:N atomic rate according to XRD analyses. Sample 1 contains two phases, but the hexagonal

phase's score is very low. The other phase is the cubic BN phase. By only changing the Ar content, cubic BN phases can be produced. In this paper, the crystal phase transition with N₂ gas concentration was shown. Considering these properties, the deposited BN film can be used for optoelectronic devices, gas sensor applications, anti-reflective coatings, and beam splitters. The obtained sample has a low SFE according to the literature.

ACKNOWLEDGEMENT

This research activity was supported by ESOGU research council (Grant numbers of 201219026).

REFERENCES:

- [1] Alemu A, Freundlich A, Badi N, Boney, C, & Bensaoula, A (2010). Low temperature deposited boron nitride thin films for a robust anti-reflection coating of solar cells. *Solar Energy Materials and Solar Cells*, 94(5), 921-923.
- [2] Anzai A, Nishiyama, F, Yamanaka, S & Inumaru, K (2011). Thin film growth of boron nitride on α -Al₂O₃ (001) substrates by reactive sputtering. *Materials Research Bulletin*, 46(12), 2230-2234.
- [3] Todi VO, Shantheyanda BP, Todi RM, Sundaram KB, & Coffey K (2011). Optical characterization of BCN films deposited at various N₂/Ar gas flow ratios by RF magnetron sputtering. *Materials Science and Engineering: B*, 176(12), 878-882.
- [4] Yang X, Li H, Li Y, Lv X, & Zou G (2010). Synthesis and optical properties of purified translucent, orthorhombic boron nitride films. *Journal of Crystal Growth*, 312(23), 3434-3437.
- [5] Jin-Xiang D, Xiao-Kang Z, Qian Y, Xu-Yang W, Guang-Hua C, & De-Yan H (2009). Optical properties of hexagonal boron nitride thin films deposited by radio frequency bias magnetron sputtering. *Chinese Physics B*, 18(9), 4013.
- [6] Yang X, Li H, Li Y, Lü X, Gao S, Zhu P, Zhang Q, Zhang TC, Zou G (2009). Dependence of RF power on the phase transformation for boron nitride films deposited on graphite at room temperature. *Journal of Crystal Growth*, 311(14), 3716-3720.
- [7] Weißmantel E., Pfeifer, T., & Richter, F. (2002). Electron microscopic analysis of cubic boron nitride films deposited on fused silica. *Thin solid films*, 408(1), 1-5.
- [8] Panayiotatos Y, Patsalas P, Charitidis C, & Logothetidis S (2002). Mechanical performance and growth characteristics of boron nitride films with respect to their optical, compositional properties and density. *Surface and Coatings Technology*, 151, 155-159.
- [9] Zhang XW, Zou YJ, Wang B, Song XM, Yan H, Chen GH, & Wong, S. P. (2001). Optical band gap and refractive index of c-BN thin films synthesized by radio frequency bias sputtering. *Journal of materials science*, 36(8), 1957-1961.
- [10] Dimitrov V & Sakka S (1996). Electronic oxide polarizability and optical basicity of simple oxides. I. *Journal of Applied Physics*, 79(3), 1736-1740
- [11] Pat S & Kokkokoglu M (2010). Characterization of deposited AlN thin films at various nitrogen concentrations by RF reactive sputtering. *OPTOELECTRONICS AND ADVANCED MATERIALS-RAPID COMMUNICATIONS*, 4(6), 855-858.

- [12] Ekem N, Korkmaz S, Pat S, Balbag M Z, Cetin N E, Ozmumcu M, Vladoiu R, Musa, G (2008). ZnO thin film preparation using RF sputtering at various oxygen contents. *Journal of Optoelectronics and Advanced materials*, 10(12), 3279-3282.
- [13] Şenay V, Pat S, Korkmaz Ş, Aydoğmuş T, Elmas S, Özen S, Ekem N, Balbağ M Z (2014). ZnO thin film synthesis by reactive radio frequency magnetron sputtering. *Applied Surface Science*, 318, 2-5.
- [14] Pat S, & Korkmaz Ş (2015). Nanostructured vanadium carbide thin films produced by RF magnetron sputtering. *Scanning*, 37(3), 197-203.
- [15] Ekem N, Korkmaz S, Pat S, Balbag M Z, Cetin E N, & Ozmumcu M (2009). Some physical properties of ZnO thin films prepared by RF sputtering technique. *International Journal of Hydrogen Energy*, 34(12), 5218-5222.
- [16] Liu Z Z, Xu F, Zhang X H, & Zuo DW (2015). Preparation of Nanocrystalline Cubic Boron Nitride Coating by Magnetron Sputtering Method. *In Key Engineering Materials* 656, 80-85.
- [17] Ulrich S, Scherer J, Schwan J, Barzen I, Jung K, Scheib M, & Ehrhardt H (1996). Preparation of cubic boron nitride films by radio frequency magnetron sputtering and radio frequency ion plating. *Applied physics letters*, 68(7), 909-911.
- [18] Lee ES., Park JK., Lee WS, Seong TY, & Baik YJ (2013). Effect of deposition temperature on cubic boron nitride thin film deposited by unbalanced magnetron sputtering method with a nanocrystalline diamond buffer layer. *Metals and Materials International*, 19(6), 1323-1326.
- [19] Tzeng Y, & Zhu H (1999). Electron-assisted deposition of cubic boron nitride by rf magnetron sputtering. *Diamond and related materials*, 8(8), 1402-1405.
- [20] Quéré D (2005). Non-sticking drops. *Reports on Progress in Physics* 68(11) 2495.